

Haptotropic Shifts in $(C_5H_5)Fe$ and $Mn(CO)_3$ Complexes of 4*H*-Cyclopenta[*def*]phenanthrene (cppH): X-ray Crystal Structure and NMR Fluxionality of $(\eta^1\text{-cpp})Mn(CO)_3(PEt_3)_2$

Andreas Decken,[†] Suzie S. Rigby, Luc Girard,[‡] Alex D. Bain, and Michael J. McGlinchey*[§]

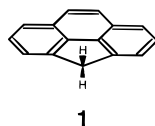
Department of Chemistry, McMaster University, Hamilton, Ontario L8S 4M1, Canada

Received September 30, 1996[⊗]

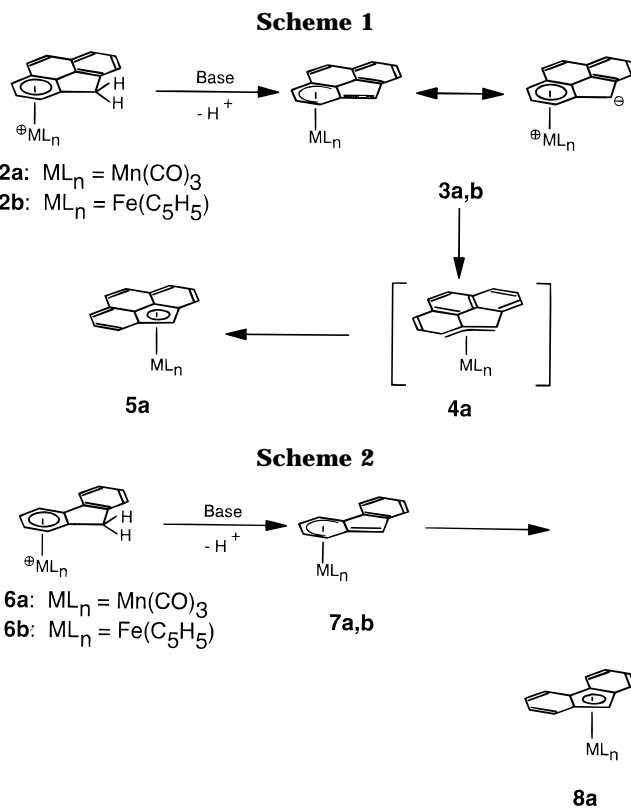
The favored pathways for the haptotropic shifts from $(\eta^6\text{-cpp})ML_n$ to $(\eta^5\text{-cpp})ML_n$, where cppH is 4*H*-cyclopenta[*def*]phenanthrene and $ML_n = Fe(C_5H_5)$ or $Mn(CO)_3$, have been investigated by means of extended Hückel molecular orbital calculations, and energy hypersurfaces for these processes have been obtained. These data suggest the intermediacy of an exocyclic $(\eta^3\text{-cpp})ML_n$ species, stabilized by the presence of a naphthalene-type 10π aromatic system. In an attempt to generate $(\eta^3\text{-cpp})Fe(CO)(C_5H_5)$, the corresponding $(\eta^1\text{-cpp})Fe(CO)_2(C_5H_5)$ complex was prepared and allowed to decompose; the major products were $[(C_5H_5)Fe(CO)_2]_2$ and the cpp trimer, $C_{15}H_8(C_{15}H_9)_2$, **20**, that was shown to adopt a rigid geometry with C_2 symmetry. Treatment of $(\eta^5\text{-cpp})Mn(CO)_3$ with triethylphosphine yields $(\eta^1\text{-cpp})Mn(CO)_3(PEt_3)_2$, **23**, which exhibits hindered rotation about the C(4)–Mn bond with a barrier of 16.5 kcal mol⁻¹. The molecule $[(\eta^6\text{-cppH})Fe(C_5H_5)]PF_6$, **2b**, and also the manganese complex **23** have been characterized by X-ray crystallography. The relevance of these (and other literature data) to the mechanisms of haptotropic shifts are discussed.

Introduction

We have recently reported the syntheses and structural characterization of a number of organometallic derivatives of the tetracyclic ligand 4*H*-cyclopenta[*def*]phenanthrene (cppH), **1**.^{1,2} Deprotonation of the $(\eta^6\text{-cppH})Mn(CO)_3]^+$ complex, **2a**, yields initially the zwitterionic species **3a**, which rapidly undergoes a haptotropic shift to give the $(\eta^5\text{-cpp})Mn(CO)_3$ isomer **5a** (Scheme 1). These data parallel the earlier observations of Treichel on the analogous fluorenyl systems **6** through **8**³ (Scheme 2). Albright, Hoffmann, and their colleagues⁴ have shown that the favored trajectory for such haptotropic shifts is not the "least-motion" pathway, whereby the ML_n fragment merely traverses the common bond



between the six- and five-membered rings, but rather involves a more circuitous route. Indeed, for the indenyl case, it was suggested that the process occurs by way of an exocyclic η^3 -transition state, analogous to **4**. This hypothesis is strongly supported by the data on cpp complexes which undergo facile haptotropic shifts (such as the transformation from **2a** to **5a**) which can



[†] Present address: Department of Chemistry, University of New Brunswick, Fredericton, NB, E3B 5A3, Canada.

[‡] Present address: Department of Chemistry and Biochemistry, Texas Tech University, Box 41061, Lubbock, TX 79409-1061.

[§] Fax: (905)-522-2509. E-mail: mcglinch@mcmaster.ca.

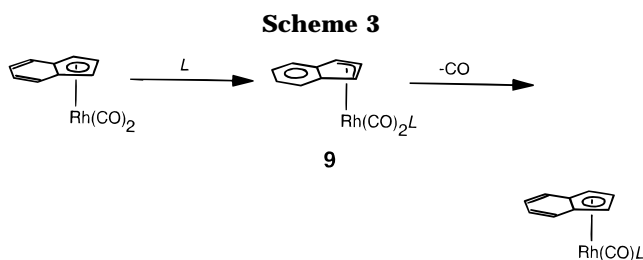
[⊗] Abstract published in *Advance ACS Abstracts*, March 1, 1997.

(1) Decken, A.; Britten, J. F.; McGlinchey, M. J. *J. Am. Chem. Soc.* **1993**, *115*, 7275.

(2) We are aware of only one other metal complex of cppH, namely [(4-methyl-isopropylbenzene)Ru(cppH)][BF₄]₂: Porter, L. C.; Polam, J. P.; Mahmoud, J. *Organometallics* **1994**, *13*, 2092.

(3) (a) Treichel, P. M.; Johnson, J. W. *Inorg. Chem.* **1977**, *16*, 749.
(b) Johnson, J. W.; Treichel, P. M. *J. Am. Chem. Soc.* **1977**, *99*, 1427.
(c) Johnson, J. W.; Treichel, P. M. *J. Chem. Soc., Chem. Commun.* **1976**, 688.
(d) Treichel, P. M.; Fivizzani, K. P.; Haller, K. J. *Organometallics* **1982**, *1*, 931.

(4) Albright, T. A.; Hoffmann, P.; Hoffmann, R.; Lilly, C. P.; Dobosh, P. A. *J. Am. Chem. Soc.* **1983**, *105*, 3396.



proceed via a naphthalene-type transition state **4a**. The 10 π aromatic character of the transition state would be expected to lower the activation energy barrier for this process. This situation is entirely analogous to the well-known “indenyl effect” whereby substitution of a ligand, L, in (η^5 -indenyl)ML_n is several orders of magnitude more rapid than for the corresponding (η^5 -cyclopentadienyl)ML_n system;⁵ the controlling factor here is the ability of the metal to undergo ring slippage into an η^3 -transition state such that the six-membered ring possesses aromatic character, as in **9** (Scheme 3).

We here describe a series of experiments designed to provide access to η^3 -cpp complexes either by loss of a ligand from an η^1 -cpp precursor or by addition of a ligand to an η^5 -system. These data are supplemented by molecular orbital calculations at the extended Hückel level which yield energy hypersurfaces for migration of organometallic fragments over a cpp framework.

Results and Discussion

Migration Pathways over a Cpp Surface. As noted above, Albright and Hoffmann have shown that, for a metal moiety undergoing a haptotropic shift between the centers of the six- and five-membered rings in the indenyl system, the least-motion pathway is not the favored route.⁴ Such a trajectory loses a major portion of the bonding interactions between the ligand and the migrating organometallic fragment. In order to carry out a comparable calculation for the haptotropic rearrangement of a (C₅H₅)Fe moiety across a C₁₅H₉ surface, we needed reliable geometric parameters on which to base the EHMO calculations. To this end, the structure of [$(\eta^6$ -cppH)Fe(C₅H₅)]⁺PF₆⁻, **2b**, was determined by a single-crystal X-ray diffraction study, and a view of the cation appears as Figure 1. The tetracyclic system deviates only slightly from planarity, and the bond distances and angles compare very favorably with those we have reported previously for (η^6 -cppH)Cr(CO)₃ and for (η^5 -cpp)Mn(CO)₃, **5a**.¹ The distances from the iron atom to the C₅H₅ and cpp ring planes are 1.668(5) and 1.564(7) Å, respectively. The synthesis of **2b** also yielded a small quantity of the bis-adduct [η^6 : η^6 -cppH-(FeCp)₂][PF₆]₂. The singlet character of the CH₂ group indicates formation of the trans isomer which possesses C₂ symmetry.

Figure 2 depicts the EHMO-calculated energy hypersurface for migration of a (C₅H₅)Fe fragment across a cpp framework. As anticipated from the previous work on indenyl and naphthalene systems,⁴ the least-motion route is strongly disfavored. The minimum energy trajectory follows a circuitous path but, even so, there is a substantial barrier (≈ 32 kcal mol⁻¹) to overcome.

(5) Crabtree, R. H. *The Organometallic Chemistry of the Transition Metals*, 2nd ed.; John Wiley: New York, 1993; pp 91–92 and references therein.

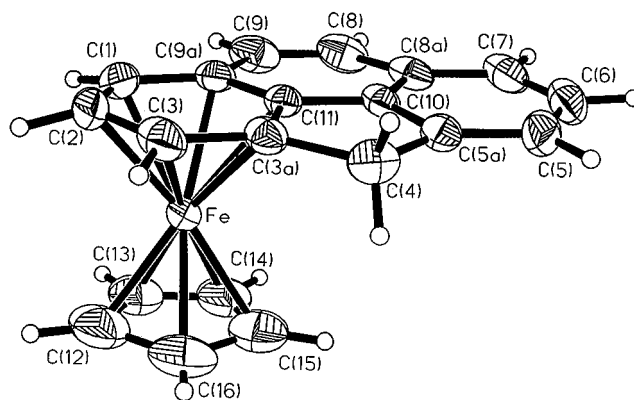


Figure 1. View of the cation in [(cpp)Fe(C₅H₅)]⁺[PF₆]⁻, **2b**, showing the atom-numbering scheme.

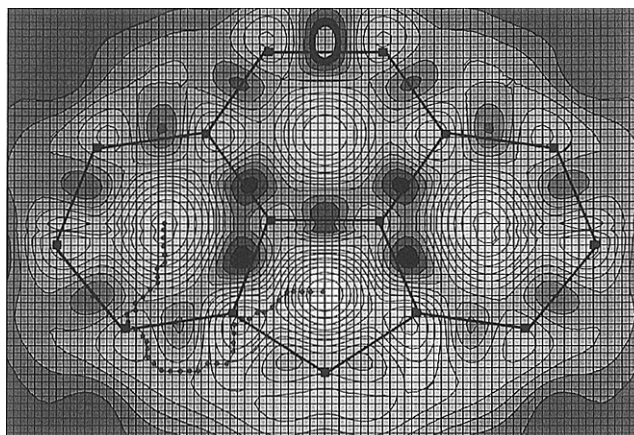


Figure 2. EHMO-calculated energy hypersurface for the migration of an Fe(C₅H₅) fragment over a C₁₅H₉ surface. The grid mesh is 0.1 Å; contour lines are incremented in units of 0.2 eV, and darker regions represent higher energies. The dotted line represents the minimum energy trajectory.

If one were to reach the exocyclic η^3 -position, the route to the η^5 -complex, **5b**, would be all downhill energetically and should be readily achievable. Experimentally, however, we have shown that deprotonation of **2b** leads only to **3b** and we have no evidence for the formation of the ferrocene analogue, (η^5 -cpp)Fe(C₅H₅), **5b**.

Calculations involving haptotropic shifts of moieties such as Mn(CO)₃ are computationally more demanding since they must take account of the orientation of the tripod.⁶ Figures 3 and 4 depict the favored route from (η^6 -cpp)Mn(CO)₃, **3a**, via (η^3 -cpp)Mn(CO)₃, **4a**, to (η^5 -cpp)Mn(CO)₃, **5a**, including the necessary rotations of the tripod during the voyage. The rate-determining step has an approximately 18 kcal mol⁻¹ barrier en route to the exocyclic η^3 -structure **4a**, after which the migration is energetically favored; indeed, (η^5 -cpp)Mn(CO)₃ is calculated to be ≈ 16 kcal mol⁻¹ more stable than the (η^6 -cpp)Mn(CO)₃ isomer.

η^3 -Indenyl and -Fluorenyl Complexes. The intermediacy of η^3 -indenyl species during ligand substitution reactions is frequently invoked. Perhaps the most dramatic illustration of the “indenyl effect” is the 10⁸-fold increase in the rate of CO substitution by a

(6) See, for example, an elegant study of how the Cr(CO)₃ group rotates as it migrates from an external ring to the central ring in starphenylene: Nambu, M.; Mohler, D. L.; Hardcastle, K.; Baldrige, K. K.; Siegel, J. S. *J. Am. Chem. Soc.* **1993**, *115*, 6138.

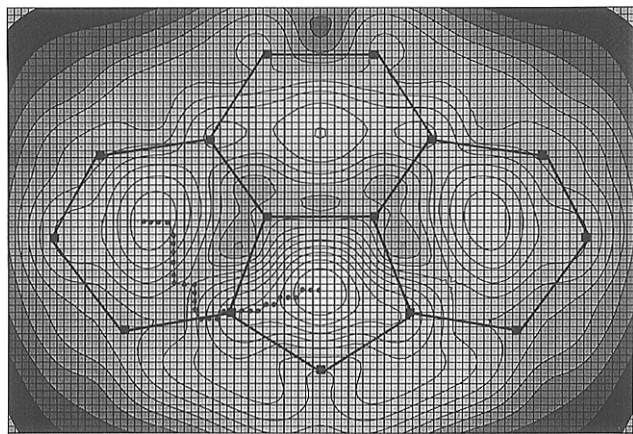


Figure 3. EHMO-calculated energy hypersurface for the migration of a $\text{Mn}(\text{CO})_3$ fragment over a C_{15}H_9 surface. The grid mesh is 0.1 Å; contour lines are incremented in units of 0.2 eV, and darker regions represent higher energies. The dotted line represents the minimum energy trajectory.

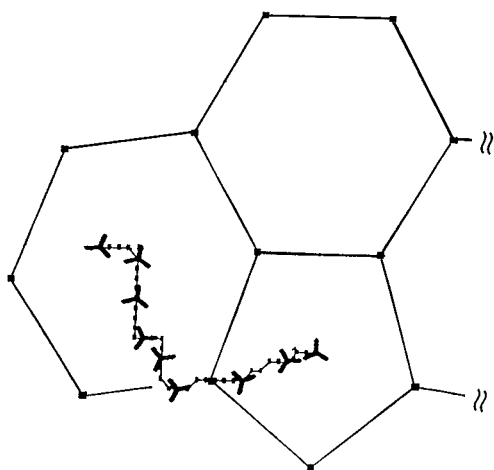
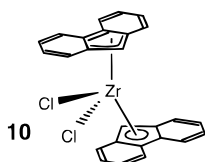


Figure 4. The EHMO-calculated minimum-energy trajectory for the migration of a $\text{Mn}(\text{CO})_3$ moiety from a peripheral six-membered ring to the five-membered ring in C_{15}H_9 showing how the orientation of the metal carbonyl tripod changes during the course of the reaction.

phosphine in $(\eta^5\text{-indenyl})\text{Rh}(\text{CO})_2$ compared to $(\eta^5\text{-C}_5\text{H}_5)\text{Rh}(\text{CO})_2$.⁷ However, only in a few cases has it been possible to characterize molecules bearing an η^3 -indenyl ligand by using NMR techniques or by single-crystal X-ray diffraction.⁸

Some years ago, the crystal structure of an apparent η^3 -fluorenyl complex was reported. In $(\text{fluorenyl})_2\text{ZrCl}_2$, **10**, the zirconium is somewhat displaced from the center



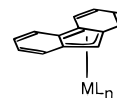
of one of the five-membered rings and could be described

(7) Rerek, M. E.; Basolo, F. *Organometallics* **1984**, *3*, 647.

(8) (a) Merola, J. S.; Kacmarcik, R. T.; Van Engen, D. *J. Am. Chem. Soc.* **1986**, *108*, 329. (b) Le Husebo, T.; Jensen, C. M. *Organometallics* **1995**, *14*, 1087. (c) Bonifaci, C.; Cecon, A.; Gambaro, A.; Ganis, P.; Santi, S.; Venzo, A. *Organometallics* **1995**, *14*, 2430. (d) Forschner, T. C.; Cutler, A. R.; Kullnig, R. K. *Organometallics* **1987**, *6*, 889. (e) Ascenso, J. A.; Gonçalves, I. S.; Herdtweck, E.; Romão, C. C. *J. Organomet. Chem.* **1996**, *508*, 169. (f) Kowalski, R. M.; Rheingold, A. L.; Trogler, W. C.; Basolo, F. *J. Am. Chem. Soc.* **1986**, *108*, 2460.

as adopting an η^3 -structure.⁹ However, this displacement appears to be primarily of steric rather than electronic origin. It has been shown by several authors, notably Marder, that in the indenyl system slippage of a metal toward an η^3 -position is accompanied by a folding of the incipient aromatic six-membered ring.¹⁰ In **10**, the " η^3 -fluorenyl" moiety retains its planarity, suggesting that the molecule is not markedly electronically perturbed.

Basolo has reported kinetic data which indicate that the replacement of a carbonyl ligand in $(\eta^5\text{-fluorenyl})\text{Mn}(\text{CO})_3$ by $\text{P}(n\text{-Bu})_3$ proceeds via $(\eta^3\text{-fluorenyl})\text{Mn}(\text{CO})_3\text{P}(n\text{-Bu})_3$, **11**.¹¹ Moreover, Wrighton has noted



11: $\text{ML}_n = \text{Mn}(\text{CO})_3\text{PBu}_3$

12: $\text{ML}_n = \text{Re}(\text{CO})_4$

that, upon irradiation of $(\eta^1\text{-fluorenyl})\text{Re}(\text{CO})_5$, an infrared-detectable intermediate is formed which is thought to be $(\eta^3\text{-fluorenyl})\text{Re}(\text{CO})_4$, **12**.¹² In both cases, the $(\eta^3\text{-fluorenyl})\text{ML}_n$ complex was assumed to adopt an endocyclic structure.

Experimental data for the isomerization of $(\eta^6\text{-fluorenyl})\text{Mn}(\text{CO})_2\text{L}$ to $(\eta^5\text{-fluorenyl})\text{Mn}(\text{CO})_2\text{L}$ are available; when $\text{L} = \text{CO}$ or R_3P , the migration barrier is found to lie in the range 23–26 kcal mol⁻¹.^{7,13} Interestingly, when L is η^1 -diphos, the activation energy drops to 20 kcal mol⁻¹, and this has been interpreted in terms of stabilization of the intermediate $(\eta^3\text{-fluorenyl})\text{Mn}(\text{CO})_2(\text{diphos})$ through coordination by the dangling phosphine.¹³

The facile occurrence of η^6 - to η^5 -haptotropic shifts upon deprotonation of metal complexes of 4*H*-cyclopenta[*def*]phenanthrene (cppH), **1**, may be attributed to the development of a 10π naphthalene-type transition state; such a phenomenon can only occur if the migrating fragment passes through an exocyclic η^3 -allylic position, as typified by **4a**. This picture gains support from the observation that, when the C(8)–C(9) double bond is selectively hydrogenated (thus destroying the potential 10π system), the migration sequence from **13** via **14** to **15** is slow, and the intermediates are readily isolated and can be fully characterized¹ (Scheme 4).

One might envisage a straightforward route to an exocyclic η^3 -cpp complex by using the synthetic methodology previously applied to $(\eta^3\text{-phenalenyl})\text{Pd}(\text{acac})$.¹⁴ However, thus far we have not been able to isolate any stable products from the reactions of cppH with palladium precursors. Instead, we chose to prepare several η^1 -cpp complexes with a view to removing a single carbonyl ligand, either by thermolysis under mild conditions or by use of Me_3NO . Consequently, the cpp⁻ anion

(9) Kowala, C.; Wunderlich, J. A. *Acta Crystallogr., Sect. B* **1976**, *32*, 820.

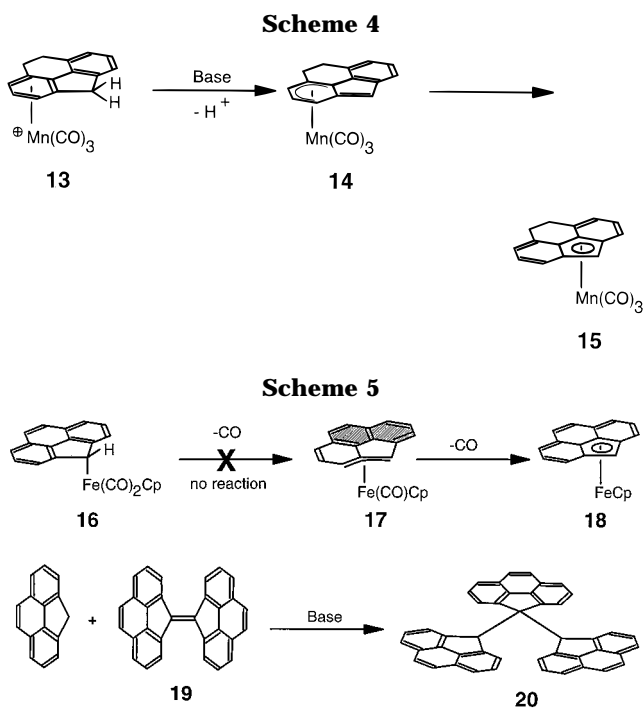
(10) Westcott, S. A.; Kakkar, A. K.; Stringer, G.; Taylor, N. J.; Marder, T. B. *J. Organomet. Chem.* **1990**, *394*, 777.

(11) Ji, L.-N.; Rerek, M. E.; Basolo, F. *Organometallics* **1984**, *3*, 740.

(12) Young, K. M.; Miller, T. M.; Wrighton, M. S. *J. Am. Chem. Soc.* **1990**, *112*, 1529.

(13) Biagioni, R. N.; Luna, A. D.; Murphy, J. L. *J. Organomet. Chem.* **1994**, *476*, 183.

(14) Nakasuji, K.; Yamaguchi, M.; Murata, I.; Tatsumi, K.; Nakamura, A. *Organometallics* **1984**, *3*, 1257.



was allowed to react with the metal carbonyl halide (C₅H₅)Fe(CO)₂I to yield the η^1 -cyp complex **16**.

Decarbonylation of (η^1 -cyp)Fe(CO)₂(η^5 -C₅H₅). The potential decarbonylation products of **16** are of considerable interest. Our original aim was the selective loss of a single carbonyl ligand to yield the exocyclic π -allyl complex **17** so as to demonstrate the viability of the proposed 10 π aromatic transition state, as in **4**. A secondary goal would be to lose both carbonyls and so generate a sandwich compound, **18** (Scheme 5). This latter molecule would be particularly interesting in view of the controversy over the status of (η^5 -fluorenyl)Fe(η^5 -C₅H₅), **8b**. Treichel has crystallographically characterized the precursor, **7b**, but found no evidence for a haptotropic shift to give **8b**.³ In contrast, Russian workers have repeatedly claimed to have isolated this fluorenyl analogue of ferrocene.¹⁵ However, these claims are based primarily on ¹H NMR and mass spectrometric measurements and, in the absence of crystallographic data, must be considered questionable.

Extended Hückel molecular orbital calculations on the series of sandwich compounds (η^5 -C₅H₅)Fe(η^5 -L), where L = cyclopentadienyl, indenyl, fluorenyl, and cyclopenta[*def*]phenanthrenyl, reveal a noticeable decrease in binding energy of the ligand L as the extra six-membered rings are added.¹⁶ Moreover, the HOMO's of the fluorenyl and cyp anions possess a large p_z coefficient at the C(4) of the five-membered ring,¹ and this may help stabilize η^1 -complexes at this position.

In an attempt to effect loss of a carbonyl ligand, (η^1 -cyp)Fe(CO)₂(η^5 -C₅H₅), **16**, was heated under reflux in

(15) Ustynyuk, N. A.; Pomazanova, N. A.; Novikova, L. N.; Kravtsov, D. N.; Ustynyuk, Yu. A. *Izv. Akad. Nauk SSSR, Ser. Khim.* **1986**, 7, 1688.

(16) The EHMO-calculated binding energies for the sandwich complexes (C₅H₅)Fe \cdots L are 75.8, 67.8, 57.6, and 57.5 eV when L = cyclopentadienyl, indenyl, fluorenyl, and cyclopenta[*def*]phenanthrenyl, respectively. In all cases the Fe–L distance was taken as 1.68 Å; for the latter two molecules, the minimum energy structure was calculated to be that whereby the (C₅H₅)Fe unit is displaced by 0.1 Å away from the center of the five-membered ring toward the unique carbon. This is in accord with the X-ray structure of (η^5 -cyp)Mn(CO)₃, **5a**, which revealed that the metal is not sited at the center of the 5-membered ring.¹

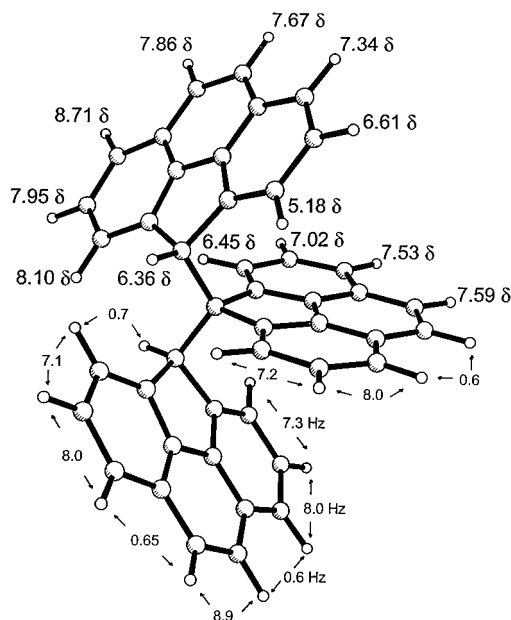


Figure 5. Energy-minimized structure for C₁₅H₈(C₁₅H₉)₂, **20**, showing the observed ¹H NMR chemical shifts and coupling constants.

toluene; however, the complex is surprisingly stable and only decomposes thermally after several hours. Similarly, treatment of **16** with Me₃NO gave only unidentified decomposition products. In contrast, when a dichloromethane solution of (η^1 -cyp)Fe(CO)₂(η^5 -C₅H₅) was left at ambient temperature for several weeks, a number of products were formed and isolated after chromatographic separation. One was readily identified as the iron dimer [(C₅H₅)Fe(CO)₂]₂, a second was the previously reported fulvalene analogue **19**,¹⁷ and the third product was shown to contain three cyp units. This latter molecule, **20**, previously prepared by treatment of the fulvalene, **19**, with cyp[−]Na⁺ (Scheme 5), was reported to exhibit (at 60 MHz) a multitude of overlapping aromatic proton NMR resonances over a surprisingly wide range of chemical shifts.¹⁷ With modern instrumentation, these peaks are more readily ascribed, and the assignments are shown in Figure 5.

A consideration of the symmetry properties of the possible structures of **20** reveals that there must be hindered rotation of the outer cyp moieties relative to the central cyp fragment. If the molecule were to adopt time-averaged C_{2v} geometry, one would expect to see eight resonances for the aromatic protons with relative intensities 2:2:2:2 (for the central C₁₅H₈ unit) and 4:4:4:4 (for the external cyp's). Experimentally, however, we observe for the aromatic protons eleven multiplets (each representing two hydrogens) plus a singlet (also two hydrogens); these aromatic resonances are spread over the range δ 8.71–5.18. A weakly coupled multiplet for the two methine protons appears at δ 6.36. These data are consistent only with a C₂ structure such that all the protons in each external C₁₅H₉ unit are non-equivalent, but each hydrogen nucleus is related to a corresponding proton in the other C₁₅H₉ moiety by rotation about a 2-fold axis. Molecular modeling, using either Alchemy¹⁸ or PC-Model,¹⁹ yields an energy-

(17) Kimura, T.; Minabe, M.; Suzuki, K. *Bull. Chem. Soc. Jpn.* **1979**, 52, 1447.

(18) ALCHEMY: available from Tripos Associates, St. Louis, MO.

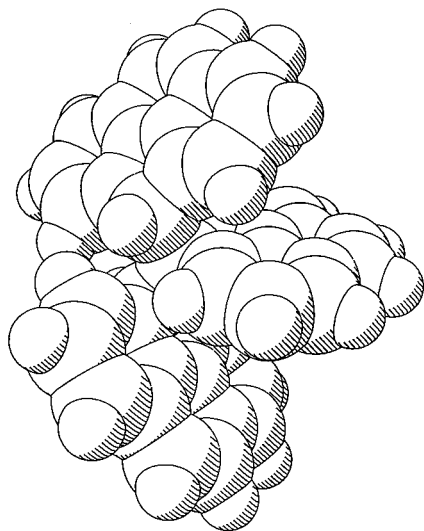


Figure 6. Space-filling model of $C_{15}H_8(C_{15}H_9)_2$, **20**, showing the crowded environment of the central cpp unit.

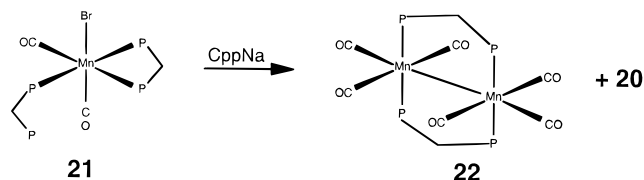
minimized C_2 structure for **20**, as shown in Figure 5. A space-filling model is depicted in Figure 6, and the interlayered character of the phenyl ring planes is apparent. One can speculate about the existence of $\pi-\pi$ interactions which may be a factor contributing to the strong red coloration of the molecule.

The enormous spread of chemical shifts for the aromatic protons in **20** arises as a result of the stacking of the phenyl rings such that certain protons are strongly influenced by the ring currents of their cpp neighbors. For example, to the extent that we choose to believe the results of the molecular modeling study, the proton which resonates at δ 5.18 lies only 2.8 Å above the center of a six-membered ring of the central $C_{15}H_8$ unit. We plan to obtain X-ray crystallographic data for **20** and to follow its molecular dynamics by 2D-EXCHANGE techniques.

Structure and Fluxional Behavior of $(\eta^1\text{-cpp})\text{-Mn}(\text{CO})_3[\text{PEt}_3]_2$. Since the reaction of the cpp anion, $C_{15}H_9^-$, with $\text{BrMn}(\text{CO})_5$ leads directly to $(\eta^5\text{-cpp})\text{-Mn}(\text{CO})_3$, with no detectable intermediacy of $(\eta^1\text{-cpp})\text{-Mn}(\text{CO})_5$ or $(\eta^3\text{-cpp})\text{-Mn}(\text{CO})_4$,¹ we chose to replace four of the carbonyl ligands by phosphines in the hope that the one remaining CO group could be selectively removed to yield an $\eta^3\text{-cpp}$ complex. It has been reported that $\text{BrMn}(\text{CO})(\text{dppm})_2$ can be prepared by UV-irradiation of $\text{BrMn}(\text{CO})_5$ in the presence of excess $\text{Ph}_2\text{PCH}_2\text{PPh}_2$; however, we were unable to obtain useful yields of the desired monocarbonyl complex. The corresponding thermal reaction yields $\text{BrMn}(\text{CO})_2(\text{dppm})_2$, **21**, in which one dppm is chelating while the other has a dangling phosphine.²⁰ When a THF solution of **21** was heated under reflux with cppNa, the products isolated were the known complex $[\text{Mn}(\text{CO})_3(\mu\text{-dppm})_2]$, **22**,²¹ and the previously discussed cpp trimer **20** (Scheme 6).

Consequently, it was decided to treat $(\eta^5\text{-cpp})\text{-Mn}(\text{CO})_3$ with triethylphosphine to see whether addition of Et_3P or replacement of one or more CO ligands occurred. The product isolated was identified mass spectrometrically

Scheme 6



as the bis(phosphine) adduct $(\eta^1\text{-cpp})\text{-Mn}(\text{CO})_3[\text{PEt}_3]_2$, **23**. This molecule is apparently the cpp analogue of



Biagioni's η^1 -fluorenyl complex **24**.²² [We note that thermolysis of $(\eta^1\text{-fluorenyl})\text{-Mn}(\text{CO})_3[\text{PEt}_3]_2$ yields 9,9'-bis(fluorenylidene), presumably by homolytic cleavage of the fluorenyl-manganese bond.²²]

In the fluorenyl system, it was noted that the ^{31}P NMR spectrum exhibited two signals, perhaps suggesting a cis orientation of axial and equatorial Et_3P ligands. However, on the basis of the observed $J(^{31}\text{P}-^{13}\text{C})$ coupling constants, Biagioni argued that the molecule was actually the trans meridional isomer but that steric crowding around the manganese locked the molecule in an unsymmetrical conformation.²² Should this also be the case for the cpp complex, **23**, one might imagine that the two ^{31}P resonances would coalesce at elevated temperatures.

In an attempt to verify Biagioni's proposal that **24** (and presumably **23**) adopted the trans meridional structure, $(\eta^1\text{-cpp})\text{-Mn}(\text{CO})_3[\text{PEt}_3]_2$ was heated to 80 °C, but decomposition was evident, even at 60 °C, before any sign of ^{31}P NMR peak coalescence was detected.²³ The other approach to measuring the activation barrier for interconversion of the ^{31}P environments involved cooling the sample until coupling between the two phosphorus environments was observed. In principle, one could calculate the rotational barrier from the line-broadening behavior of the two ^{31}P doublets. In practice, however, $J(^{31}\text{P}-^{31}\text{P})$ was found to be only 15 Hz and so only an approximate value of ΔG^\ddagger could be obtained. Consequently, we chose to use a two-dimensional NMR exchange method to probe this barrier. Figure 7 shows the results of a 2D-EXSY experiment for the ethyl protons of the Et_3P ligands in **23**.

With a short mixing time ($\tau_m = 25$ ms) no off-diagonal cross-peaks are detectable; however, when τ_m is 50 ms, magnetization transfer between the two sets of methylene protons and between the two methyl environments is evident. This process can be quantified by means of a series of selective inversion experiments²⁴ to determine exchange rates, at different temperatures, between the two methylene signals. These data yielded an Eyring plot from which the following values were

(19) PC-MODEL, June 1990 version: available from Dr. K. Gilbert, Serena Software, Bloomington, IN.

(20) Reimann, R. H.; Singleton, E. *J. Organomet. Chem.* **1972**, *38*, 113.

(21) King, R. B.; Raghuvver, K. S. *Inorg. Chem.* **1984**, *23*, 2482.

(22) Biagioni, R. N.; Lorkovic, I. M.; Skelton, J.; Hartung, J. B. *Organometallics* **1990**, *9*, 547.

(23) On a 300 MHz instrument the ^{31}P environments in **23** are separated by 461.5 Hz; a coalescence temperature of 90 °C would correspond to a ΔG^\ddagger value of 16.5 kcal mol⁻¹.

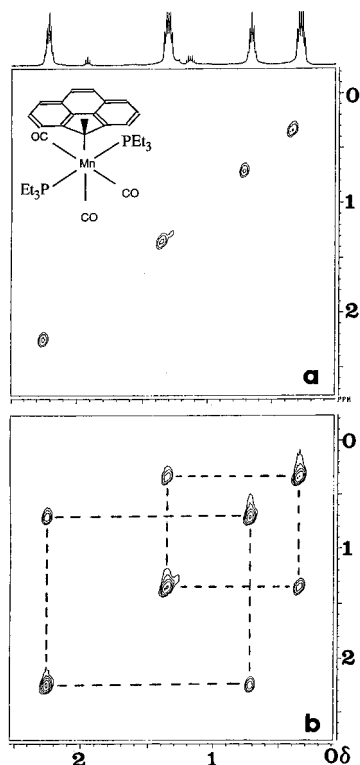


Figure 7. 2D-EXSY spectra of (η^1 -cpp)Mn(CO)₃(PEt₃)₂, **23**, recorded at 30 °C in CD₂Cl₂, with mixing times, τ_m , of (a) 25 ms and (b) 50 ms.

extracted: $\Delta H^\ddagger = 13.1 \pm 0.2$ kcal mol⁻¹, $\Delta S^\ddagger = -11.2 \pm 0.7$ eu, and $\Delta G^\ddagger_{300} = 16.5 \pm 0.2$ kcal mol⁻¹. This process must involve rotation about the C(4)–Mn single bond which brings about equilibration of the two different Et₃P environments. It is noteworthy that the methine hydrogen at C(4) of the cpp fragment maintains its coupling to both phosphorus nuclei at all temperatures; consequently, the process must be intramolecular and exchange between bound and free triethylphosphine can be ruled out.

The demonstrated interconversion of the two Et₃P environments in (η^1 -cpp)Mn(CO)₃[PEt₃]₂ is in complete accord with Biagioni's postulate of a trans meridional arrangement of the phosphine ligands at manganese in the fluorenyl analogue **24**. The structure of the cpp complex **23** was confirmed by a single-crystal X-ray diffraction study. As shown in Figure 8, the phosphines are indeed trans meridional and the P–Mn–P vector is aligned such that it makes an angle of 35° with the mirror plane passing through C(4) and the midpoint of the C(8)–C(9) bond in cpp. The ethyl substituents on each phosphorus adopt propellor-like conformations, and this results in almost perfect C₂ local symmetry for the Mn(CO)₃[PEt₃]₂ fragment.

To understand the fluxional behavior of **23**, we used the crystallographic data to provide a starting point for

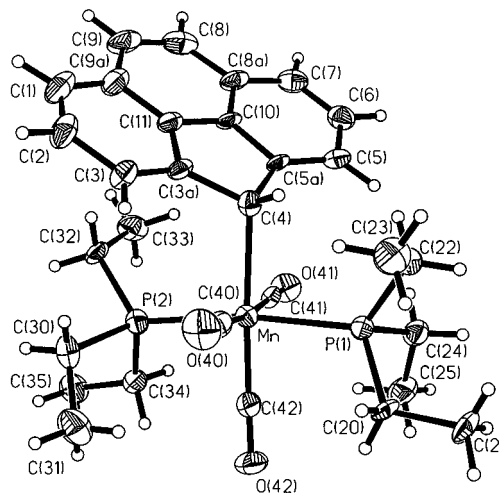


Figure 8. View of (η^1 -cpp)Mn(CO)₃(PEt₃)₂, **23**, showing the atom-numbering scheme.

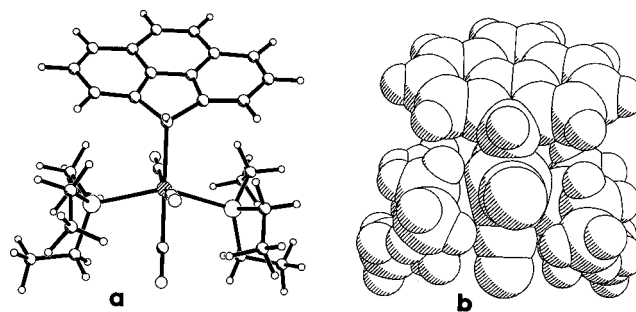


Figure 9. Energy-minimized structure for (η^1 -cpp)Mn(CO)₃(PEt₃)₂, **23**, constrained such that the P–Mn–P unit straddles the cpp mirror plane, as in the transition state for phosphine equilibration: (a) ball-and-stick model; (b) space-filling representation.

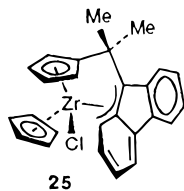
a molecular modeling study of the structure of the transition state through which the phosphine ligands could interconvert. Gratifyingly, the globally minimized geometry given by PC-Model corresponded very well to the X-ray crystal structure. To model the transition state through which phosphine equilibration could occur, the molecule was constrained such that the P–Mn–P fragment straddled the mirror plane which bisected the η^1 -cpp ligand. The PC-Model minimized structure allowed the ethyl substituents to adopt their most favorable orientations, and this conformation is shown in Figure 9a. The space-filling representation in Figure 9b illustrates how the steric problems arise as the result of the hydrogens at C(3) and C(5) protruding into the cone angle swept out by the triethylphosphine.

To conclude, EHMO calculations have been carried out to estimate the barriers toward haptotropic shifts of (C₅H₅)Fe or Mn(CO)₃ moieties over the surface of the tetracyclic cyclopentanophenanthrenyl system. These data indicate that the trajectories for such migrations involve an η^3 -exocyclic structure which maintains the 10 π electron (naphthalene-type) character of the transition state. Attempts to isolate η^3 -cpp intermediates by selective ligand loss from η^1 -cpp precursors gave decomposition products, including the cpp trimer, **20**, which exhibits a remarkable range of aromatic proton shifts in its ¹H NMR spectrum. Moreover, (η^1 -cpp)Mn(CO)₃[PEt₃]₂, **23**, shows restricted rotation about the cpp–Mn σ -bond, and the barrier for this fluxional

(24) (a) Grassi, M.; Mann, B. E.; Pickup, B. T.; Spencer, C. M. *J. Magn. Reson.* **1986**, *69*, 92. (b) Led, J. J.; Gesmar, H. *J. Magn. Reson.* **1982**, *49*, 444. (c) Muhandiram, D. R.; McClung, R. E. D. *J. Magn. Reson.* **1987**, *71*, 187. (d) Bain, A. D.; Cramer, J. A. *J. Magn. Reson.* **1993**, *A103*, 217. (e) Rigby, S. S.; Girard, L.; Bain, A. D.; McGlinchey, M. J. *Organometallics* **1995**, *14*, 3798. (f) Forsén, S.; Hoffman, R. A. *J. Chem. Phys.* **1963**, *39*, 2982. (g) Forsén, S.; Hoffman, R. A. *J. Chem. Phys.* **1964**, *40*, 1189. (h) Hoffman, R. A.; Forsén, S. *J. Chem. Phys.* **1966**, *45*, 2049. (i) Sanders, J. K. M.; Hunter, B. K. *Modern NMR Spectroscopy, A Guide for Chemists*; Oxford University Press: Oxford, U.K., 1987; pp 224–234.

process has been evaluated by selective inversion NMR spectroscopy. The X-ray structure of **23** supports Biagioni's postulate that such systems adopt a trans meridional geometry.

Epilogue. Although our "rational" routes to (η^3 -cpp)-ML_n complexes have not yet yielded isolable molecules, we were gratified to see that a closely analogous system was recently obtained serendipitously by Green *et al.* in the course of their studies on *ansa*-zirconocenes.²⁵ The X-ray structure of [$(\eta^5$ -C₅H₄)CMe₂(η^3 -C₁₃H₈)Zr(η^5 -C₅H₅)-Cl, **25**, shows clearly that the η^3 -fluorenyl ligand is



attached in an exocyclic fashion. As we have discussed at some length already, such a bonding mode allows one of the six-membered rings of the fluorenyl ligand to retain its 6 π aromatic character and so provides strong support for the predicted pathway of η^6 - to η^5 -haptotropic shifts across polycyclic surfaces.

Experimental Section

All syntheses were carried out under a dry nitrogen atmosphere utilizing conventional benchtop and glovebag techniques. Solvents were dried and distilled according to standard procedures.²⁶ ¹H and ¹³C NMR spectra were recorded on a Bruker AM-500 spectrometer operating at 500 and 125.72 MHz, respectively. ³¹P NMR spectra were obtained on a Bruker AC-300 spectrometer operating at 121.442 MHz. Selective inversion experiments were carried out as described previously.^{24e} Fast atom bombardment (FAB) mass spectra were obtained on a VG ZAB-E spectrometer. 3-Nitrobenzyl alcohol was used as the sample matrix, and xenon was the bombarding species (8 keV). Microanalytical data are from Guelph Chemical Laboratories, Guelph, Ontario, Canada.

[$(\eta^6$ -4H-Cyclopenta[def]phenanthrene)Fe(C₅H₅)PF₆, **2b.** By analogy to the general procedure of Helling and Hendrickson,²⁷ cppH (0.95 g, 5 mmol), Cp₂Fe (0.94 g, 5 mmol), aluminum powder (0.135 g, 5 mmol), and AlCl₃ (1.335 g, 10 mmol) were heated in 10 mL of decalin at 140 °C for 4 h. The mixture was cooled to 0 °C, 25 mL of water was added, and the inorganic solids were removed on a sintered funnel. The aqueous layer was isolated and extracted with ether (2 × 25 mL) and then treated with NH₄PF₆ (2 g, 12.5 mmol) in 5 mL of water. The precipitate was collected on a sintered funnel and dried under high vacuum to yield a brown solid (0.52 g, 1.44 mmol, 23% based on cppH), decomposing at 143 °C. ¹H NMR (CD₂Cl₂): δ 8.09 (d, 9.2 Hz, 1H), 7.79 (d, 9.2 Hz, 1H) (*H*-8,9), 7.92 (m, 2H), 7.88 (d, 6.2 Hz, 1H) (*H*-5,6,7), 6.93 (d, 5.7 Hz, 1H), 6.81 (d, 5.7 Hz, 1H) (*H*-1,3), 6.19 (t, 5.7 Hz, 1H) (*H*-2), 5.12 (d, 21.9 Hz, 1H), 4.69 (d, 21.9 Hz, 1H) (*H*-4), 4.29 (s, 5H) (*Cp*-ring). ¹³C NMR (acetone-*d*₆): δ 133.5, 131.8, 129.8, 126.1, 125.7, 93.3, 85.1, 84.1 (*aromatic CH*'s), 77.8 (*Cp*-ring), 142.8, 137.8, 105.9, 100.4 (*ring junction C*'s), 39.4 (*C*-4). Mass spectrum (FAB+) [*m/z* (%): 311 (100), ((C₁₅H₁₀)FeCp)⁺; 189 (14), (C₁₅H₉)⁺. Anal. Calcd for C₂₀H₁₅F₆FeP: C, 52.66, H, 3.32. Found: C, 52.77, H, 3.16. Traces of a second product were

identified as [(*trans*- η^6 : η^6 -4H-cyclopenta[def]phenanthrene)-(FeC₅H₅)₂](PF₆)₂. ¹H NMR (acetone-*d*₆): δ 8.05 (s, 2H) (*H*-8,9), 7.49 (d, 6.0 Hz, 2H), 6.89 (d, 6.0 Hz, 2H) (*H*-1,7-*H*-3,5), 6.30 (t, 6.0 Hz, 2H) (*H*-2,6), 5.62 (s, 2H) (*H*-4), 4.84 (s, 10H) (*Cp*-rings).

(η^1 -Cyclopenta[def]phenanthrenyl)Fe(CO)₂(η^5 -C₅H₅), **16.** 4H-Cyclopenta[def]phenanthrene (cppH, **1**) (570 mg, 3 mmol) and NaH (72 mg, 3 mmol) were heated to reflux in THF (10 mL) for 20 h. (η^5 -C₅H₅)Fe(CO)₂I (912 mg, 3 mmol) in THF (10 mL) was added and the reaction mixture stirred at room temperature for 4 h. The solvent was removed under reduced pressure and the products were separated by flash chromatography on silica using 2:1 hexane/CH₂Cl₂ to yield **16** (222 mg, 0.61 mmol, 20%) as an orange solid. ¹H NMR (acetone-*d*₆): δ 7.79 (s, 2H), 7.70–7.57 (m, 6H), 4.78 (s, 1H), 4.09 (s, 5H). ¹³C NMR (acetone-*d*₆): δ 218.1 (Fe–CO), 156.7, 139.0, 128.9 (*ring junction C*'s), 127.6, 126.2, 120.8, 120.7 (*aromatic C*'s), 87.6 (C₅H₅), 23.2 (C-4). IR (CH₂Cl₂): ν_{CO} at 2009 (vs) and 1956 (s) cm⁻¹. Mass spectrum (DEI+) [*m/z* (%): 366 (0.5) ([M]⁺), 338 (0.5) ([M – CO]⁺), 310 (3) ([M – 2CO]⁺), 253 (6) ([C₂₀H₁₃]⁺), 189 (100) ([C₁₅H₉]⁺), 121 (8) ([C₅H₅Fe]⁺). Anal. Calcd for C₂₂H₁₄FeO₂: C, 72.13; H, 3.83. Found: C, 72.24; H, 3.91.

Flash chromatography also gave traces of (C₅H₅)₂Fe₂(CO)₄, as well as (C₁₅H₈)₂, **19**: ¹H NMR (acetone-*d*₆) δ 8.03 (d, 8.0 Hz of d, 0.7 Hz, 2H), 7.88 (s, 2H), 7.78 (d, 7.0 Hz of d, 0.7 Hz, 2H), 7.66 (d, 8.0 Hz of d, 7.0 Hz, 2H). Mass spectrum (DEI+) [*m/z* (%): 376 (50) ([M]⁺), 189 (100) ([C₁₅H₉]⁺).

Finally, (C₁₅H₉)₂C₁₅H₈, **20**, was obtained in trace quantities as red crystals. After several repetitions of the reaction, sufficient quantity of **20** was obtained to allow the ¹H NMR spectrum to be obtained in CD₂Cl₂; these data are depicted in Figure 5. ¹³C NMR (CD₂Cl₂): δ 145.8, 143.2, 142.8, 137.9, 137.8, 128.6 (*ring junction C*'s); 127.8, 127.6, 127.0, 126.7, 125.8, 125.4, 125.3, 124.6, 124.0, 123.1, 121.2, 120.5 (*aromatic CH*'s), 62.1, 56.1. Mass spectrum (DEI+) [*m/z* (%): 567 (8) ([M + H]⁺), 377 (100) ([C₁₅H₈ – C₁₅H₉]⁺), 189 (28) ([C₁₅H₉]⁺).

(η^1 -Cyclopenta[def]phenanthrenyl)Mn(CO)₃(PEt₃)₂, **24.** (η^5 -Cp)Mn(CO)₃ (43 mg, 0.13 mmol) in benzene (2 mL) was treated with PEt₃ (150 mg, 1.27 mmol), and the color changed from red to yellow within minutes. The mixture was stirred for 5 min and concentrated to 0.5 mL, and hexane (5 mL) was added. The oily liquid was chilled at –20 °C overnight. The solvent was then decanted and the yellow solid dried in vacuum to give **24** (32 mg, 0.057 mmol; 44%). ¹H NMR (CD₂Cl₂): δ 7.83 (s, 2H), 7.80 (d, 7.0 Hz, 2H), 7.65 (d, 7.5 Hz, 2H), 7.61 (d, 7.0 Hz of d, 7.5 Hz, 2H), 4.56 (d, 8.0 Hz of d, 8.2 Hz, 1H), 2.25 (d, 7.5 Hz of q, 7.5 Hz, 6H), 1.36 (t, 7.5 Hz of d, 14.2 Hz, 9H), 0.72 (d, 7.7 Hz of q, 7.7 Hz, 6H), 0.36 (t, 7.7 Hz of d, 14.8 Hz, 9H). ¹³C NMR (CD₂Cl₂, –30 °C): δ 223.7 (d, 19.7 Hz of d, 19.7 Hz, *equatorial CO*'s), 222.6 (d, 20.3 Hz of d, 20.3 Hz, *axial CO*); 156.7, 137.5, 127.7 (*ring junction C*'s); 125.7, 125.1, 118.3, 117.7 (*aromatic C*'s); 26.4 (d, 7.5 Hz of d, 8.9 Hz) (C4); 19.5 (d, 21.4 Hz), 18.3 (d, 21.2 Hz) (*methylene C*'s); 7.6, 6.5 (*methyl C*'s). ³¹P NMR (CD₂Cl₂, –30 °C): δ 46.5 (d, 14.5 Hz), 42.7 (d, 14.5 Hz). IR (CH₂Cl₂): ν_{CO} 1999 (w), 1913 (s), 1883 (m) cm⁻¹. Mass spectrum (FAB+) [*m/z* (%): 375 (29) ([Mn(PEt₃)₂(CO)₃]⁺), 319 (43) ([Mn(PEt₃)₂(CO)]⁺), 328 (62) ([cppH]-Mn(CO)₃]⁺), 291 (100) ([Mn(PEt₃)₂]⁺), 173 (50) ([Mn(PEt₃)]⁺), 119 (66) ([HPEt₃]⁺).

X-ray Crystal Structure Determinations for **2b and **23**.** Crystal data and refinement parameters are collected in Table 1. All crystals were grown by vapor diffusion techniques²⁸ using 1,2-dichloroethane and *n*-heptane at –22 °C. The crystals were mounted on fine glass fibres with epoxy cement. The unit cells were determined by automatic indexing of 25 centered reflections. Intensity data for **2b** and **23** were collected on a Siemens P4 diffractometer fitted with a rotating anode using graphite-monochromated Mo K α X-radiation (λ = 0.710 73 Å) at room temperature. Three check reflections

(25) Diamond, G. M.; Green, M. L. H.; Mountford, P.; Popham, N. A.; Chernega, N. *J. Chem. Soc., Chem. Commun.* **1994**, 103.

(26) Perrin; D. D.; Armarego, W. L. F.; Perrin, D. R. *Purification of Laboratory Chemicals*; Pergamon Press: New York, 1980.

(27) Helling, J. F.; Hendrickson, W. A. *J. Organomet. Chem.* **1977**, *141*, 99.

(28) Stout, G. H.; Jensen, L. H. *X-ray Structure Determination*, 2nd ed.; John Wiley: New York, 1989; p 76.

Table 1. Crystallographic Data for Compounds 2b and 23

	compd	
	2b	23
formula	C ₂₀ H ₁₅ F ₆ FeP	C ₃₀ H ₃₉ MnO ₃ P ₂
fw	456.14	564.49
cryst size, mm	0.25 × 0.40 × 0.70	0.40 × 0.30 × 0.15
temp, K	300(2)	300(2) K
wavelength, Å	0.710 73	0.710 73
cryst syst	monoclinic	monoclinic
space group	P2 ₁ /c	P2 ₁ /c
a, Å	7.619(1)	16.277(3)
b, Å	16.558(2)	14.448(3)
c, Å	14.346(2)	13.216(3)
β, deg	102.00(1)	109.57(3)
V, Å ³	1770.3(4)	2928.5(11)
Z	4	4
d _{calc} , g/cm ³	1.711	1.280
μ, cm ⁻¹	10.05	05.88
F(000)	920	1192
θ range, deg	2.73–27.55	2.66–24.99
scan type	θ–2θ	θ–2θ
index ranges	0 ≤ h ≤ 9 0 ≤ k ≤ 21 –18 ≤ l ≤ 18	–19 ≤ h ≤ 18 –17 ≤ k ≤ 1 –1 ≤ l ≤ 7
no. of data colld	4399	4302
no. of unique data	4089	3293
	[R(int) = 0.0144]	[R(int) = 0.0378]
GOF ^a	1.189	1.017
R1 [I > 2σ(I)] ^a	0.0489	0.0498
wR2 ^a	0.1139	0.1100

^a $wR2 = (\sum [w(F_o^2 - F_c^2)^2] / \sum [wF_o^4])^{1/2}$. $R1 = \sum ||F_o| - |F_c|| / \sum |F_o|$. $GOF = [\sum w(F_o^2 - F_c^2)^2 / (n - p)]^{1/2}$, where n is the number of reflections and p is the number of parameters refined.

were measured every 97 reflections. The heavy atom positions were obtained using Patterson methods, and phase extension and Fourier difference techniques revealed the remaining non-hydrogen atoms. Hydrogen atoms for **2b** and **23** were included in calculated positions ($d(C-H) = 0.96$ Å) and refined using a riding model and common isotropic temperature factors. Scattering factors were supplied by the software. Data reduction, structure solution, refinement, graphics, and table generation programs are contained in the SHELXTL-PLUS program library.²⁹

Molecular orbital calculations were performed within the extended Hückel formalism using weighted H_{ij} values.³⁰ Computations were carried out by use of the program CACAO.³¹ The molecular geometries were idealized, planar versions taken from the X-ray crystal structures of $[(\eta^6\text{-cppH})\text{Fe}(\text{C}_5\text{H}_5)]^+\text{PF}_6^-$, **2b**, and of $(\eta^5\text{-cpp})\text{Mn}(\text{CO})_3$, **5a**. The following distances were used: Fe–Cp = 1.66 Å, Fe–cpp = 1.59 Å, Mn–cpp = 1.82 Å, and Mn–CO = 1.79 Å. Orbital parameters were taken from ref 4. To generate the energy hypersurfaces, the ML_n coordinates were sequentially incremented in units of 0.1 Å, as previously described in our earlier trajectory calculations.³² Moreover, for the migration of the Mn(CO)₃ group over cpp, the tripod was rotated in 10° intervals for each point on the surface, and the minimum energy value was extracted in each case.

Acknowledgment. Financial support from the Natural Sciences and Engineering Council of Canada and the donors of the Petroleum Research Fund, administered by the American Chemical Society, is gratefully acknowledged. A.D. was the recipient of a McMaster University Centennial Scholarship and was an Ontario Graduate Scholar. Mass spectra were obtained courtesy of Dr. Richard Smith of the McMaster Regional Centre for Mass Spectrometry. Finally we thank Dr. Carlo Mealli, CNR, Florence, Italy, for providing CACAO Version 4.0.

Supporting Information Available: Tables listing bond lengths and angles, atom coordinates and displacement coefficients, and X-ray parameters for **2b** and **23** (18 pages). Ordering information is given on any current masthead page.

OM960829F

(29) Sheldrick, G. M. SHELXTL PC, Release 4.1; Siemens Crystallographic Research Systems, Madison, WI 53719, 1990.

(30) (a) Hoffmann, R. *J. Chem. Phys.* **1963**, *39*, 1397. (b) Hoffmann, R.; Lipscomb, W. N. *J. Chem. Phys.* **1962**, *36*, 2179, 3489. (c) Ammeter, J. H.; Bürgi, H.-B.; Thibeault, J. C.; Hoffmann, R. *J. Am. Chem. Soc.* **1978**, *100*, 3686.

(31) Mealli, C.; Proserpio, D. M. *J. Chem. Educ.* **1990**, *67*, 3399.

(32) (a) Girard, L.; Lock, P. E.; ElAmouri, H.; McGlinchey, M. J. *J. Organomet. Chem.* **1994**, *478*, 189. (b) Ruffolo, R.; Decken, A.; Girard, L.; Gupta, H. K.; Brook, M. A.; McGlinchey, M. J. *Organometallics* **1994**, *13*, 4328.